Jurnal Ilmu Kelautan **P-ISSN: 2460-0156**
SPERMONDE (2026) 12(1): 34-47 **E-ISSN: 2614-5049**

MAPPING MANGROVE GREEN BELTS IN AQUACULTURE PONDS USING GOOGLE EARTH ENGINE

Muhammad Banda Selamat[1*], Supriadi[1], Chair Rani[1] and Amir Hamzah Muhiddin[1]

Submitted: 28 February 2026 Accepted: April 29, 2026

[1]Departemen of Marine Science, Faculty of Marine Science and Fisheries, University Hasanuddin
Corresponding Author:
*Muhammad Banda Selamat
E-mail: mbandaselamat@unhas.ac.id

ABSTRACT

Mangrove ecosystems function as vital biophysical buffers, attenuating wave energy, reducing coastal erosion, and stabilizing shorelines. Historically, they have been employed as natural barriers to protect coastal aquaculture, including fish ponds. This study examines the temporal dynamics of mangroves safeguarding the Unhas Bojo educational fish ponds using cloud-based geospatial analysis via Google Earth Engine (GEE). Field data were collected from June 2–5, 2023, across 27 sampling points within three stations, complemented by Sentinel-2A imagery (474 scenes, from 2016 to 2023). Equipment included GPS logger, quadrat, compass, ImageJ, timestamp camera, protractor, Google My Maps, GPX Viewer, QGIS, and GEE. Species identified were Rhizophora mucronata, Rhizophora apiculata, and Sonneratia alba. Average canopy cover was 76.2 ± 5.8%, indicating good ecological condition. NDVI values ranged from -0.12 to 0.65, with a model coefficient of determination (R^2) of 0.835 and RMSE of 1.69. Despite overall resilience, seasonal NDVI dynamics revealed consistent patterns: higher productivity during the dry season and reduced values in the rainy season. These intra-annual fluctuations demonstrate that mangrove vigor is strongly coupled with climatic drivers, particularly rainfall intensity and hydrological regimes. Persistent canopy cover underscores ecological resilience, yet sensitivity to seasonal stressors highlights the importance of monitoring mangrove health under variable climatic conditions.

Keywords: mangrove, mapping, NDVI, GEE, Bojo

INTRODUCTION

Mangroves are vegetation that live and occupy the outermost line of the coastline that is regularly inundated by seawater. The increase in human activities in coastal areas, including aquaculture, has been a significant factor contributing to the decline of mangrove ecosystems in these regions. In many places, mangroves are still maintained merely to help prevent the embankments that form the boundaries of ponds from eroding easily and to better manage seawater circulation. This effort is far cheaper and more sustainable compared to building concrete retaining walls (Bosma et. al., 2020).

Mangroves as pond protectors play a role in damping the energy of sea waves and sediment accumulation, thereby strengthening pond embankments facing the sea. Traditional cultivators can also collect fish or shrimp seedlings from the existing mangrove ecosystem to stock their ponds. Another known function of mangroves is that their roots have the ability to absorb heavy metals, and their leaf litter can enhance nutrient cycling and macrobenthic diversity. (Naylor et. al., 2000).

Satellite remote sensing provides comprehensive spatial data for inaccessible regions, making it valuable for mangrove studies (Diaz & Blackburn, 2003). The European Space Agency's Copernicus program, operational since 2012, deploys Sentinel satellites for environmental monitoring. Sentinel-2A and 2B deliver high-resolution multispectral imagery, enabling NDVI calculation from bands 8 and 4. NDVI has been widely applied to assess vegetation health in spatial planning, forest and water management, agriculture, and food security. (https://sentiwiki.copernicus.eu/web/s2-applications).

An index is a number that characterizes the intensity of an event that is too complex to be broken down into known variables (Bannari et. al., 1995). Two or more bands in a multispectral system can be transformed to form a new image to extract spatial information. The resulting image can highlight certain objects on the Earth, such as vegetation. More than a hundred vegetation indices have been created from multispectral images (Xue and Su, 2017). The Normalized Difference Vegetation Index (NDVI) is one of the earliest remote sensing image indices used to simplify the complexity of multispectral imagery. NDVI can be generated from any multispectral sensor that has visible and near-infrared bands. NDVI has now become the most popular index used for vegetation assessment, including mangroves.

Google Earth Engine (GEE) is a computing platform that allows users to perform geospatial analysis on cloud infrastructure. Earth Engine has a publicly accessible data catalog that includes various satellite imagery data, such as Sentinel-2,

Landsat, MODIS, and various derived spatial data. GEE features a Code Editor designed to make complex geospatial workflows easier and faster (https://earthengine.google.com/).

Most mangrove monitoring emphasizes conservation areas or natural forests and relies on static NDVI snapshots (Tran et al., 2022; Win & Sasaki, 2024). Aquaculture-linked mangroves, such as those protecting educational fish ponds, remain underrepresented. While regional studies exist (Jamaluddin et al., 2022; Ruan et al., 2022; Furusawa et al., 2023), site-specific, long-term datasets for small-scale, educationally managed aquaculture systems are scarce, leaving a gap in localized ecological insights.

This study aims to assess the temporal dynamics of mangrove condition in the educational aquaculture ponds at Bojo, Hasanuddin University. Condition parameters were derived from Normalized Difference Vegetation Index (NDVI), computed using cloud-based geospatial analysis on the Google Earth Engine platform, and integrated with rainfall data spanning from year 2017 to 2023.

MATERIALS AND METHODS

Time and Location

This study is located at the Education Aquaculture Pond of Hasanuddin University, at Bojo Village, Mallusetasi District, Barru Regency, South Sulawesi. The study site is approximately 136 km from the university campus, toward northside of Makassar.

Field observations were conducted from 2 to 5 June 2023. The mangrove area under study encompassed approximately 2.75 hectares, with a perimeter of about 1,300 meters. Sampling design was structured into three stations, each subdivided into three plots with three replicates to enhance spatial representativeness and statistical robustness. The spatial distribution of sampling points is illustrated in Figure 1.

Figure 1. The study location is in the mangrove area within the Unhas educational pond area in Bojo Village, Mallusetasi, Barru Regency. The sampling plot is indicated by the red box.

Material and Equipment

Equipment used in the field includes sieves-net, quadrants, shovels, measuring tapes, and sample bags. Software used for data collection includes GPS loggers, timestamp cameras, and protractors. Laboratory equipment used includes trays, magnifying glasses, and benthos identification books. Software for data analysis includes the Image J application, Google My Maps, GPX Viewer, QGIS, and the Google Earth Engine (GEE) web browser.

Sentinel-2 Image Dataset and Rainfall

The Sentinel 2A satellite image dataset analyzed online comes from the Earth Engine data catalog. It is available in the cloud at https://developers.google.com/earth-engine/datasets/catalog/sentinel-2. The dataset used for this study consists of 474 images, recorded from September 12, 2016, to December 30, 2023. Long-term mangrove studies require consistent data. Applying a <10% cloud cover filter reduces atmospheric interference, ensuring reliable seasonal comparisons. The COPERNICUS/S2 collection provides Level-1C images that are radiometrically and geometrically corrected, including ortho-rectification and global coordinate adjustment with sub-pixel accuracy. Pixel values represent Top of Atmosphere (TOA) reflectance, and the dataset includes 13 multispectral bands plus 3 quality assurance bands (ESA, 2015).

Rainfall data for this study were obtained from BPS Mallusetasi figures published between 2016 and 2023 (BPS, 2023). The tables were re-tabulated to presented as a bar plot graph.

Google Earth Engine script for NDVI mapping

NDVI mapping from Sentinel-2 imagery was conducted using the Google Earth Engine (GEE) platform. The programming script is provided in Appendix 1, while the general image processing workflow in GEE is summarized in Table 1.

Table 1. The step-by-step explanation of mapping NDVI using GEE script

Step of work	Script example	Function
Displaying ROI (Region of Interest)	Map.addLayer(geometry) dan Map.centerObject(geometry)	Shows the study area on the map and centers the view on it
Filtering the image collection	ee.ImageCollection('COPERNICUS/ S2')	Calls the Sentinel-2 dataset (COPERNICUS/S2). Filters by date range (2016–2023), ROI, and cloud cover < 10%.
Creating median composites	filtered.median() dan clip(geometry)	Generates median composites for year 2016 to 2023 and clips to the ROI
Calculating NDVI	normalizedDifference(['B8','B4'])	Computes NDVI = (NIR – RED) / (NIR + RED). Adds NDVI as a new band to each image in the collection.
Creating a time series chart	ui.Chart.image.series(...)	Displays NDVI temporal variation across the study period.
Visualizing NDVI Composite	Map.addLayer(ndviComposite, addNDVI, 'ndvi')	Displaying an NDVI map with a color scale (palette) from low to high
Visualizing RGB and False-Color Composites	Map.addLayer(...,{bands:['B4','B3','B 2']}, "Natural-colour")	Displaying RGB composite images (natural color) and false color for vegetation interpretation.

Mangrove species, Canopy Cover, and NDVI

Mangrove species were observed within three square plots measuring 100 square meters for each station. Individuals mangrove found within the plots were censused and classified as trees, stands, and seedlings. Mangrove species identification was carried out based on the observation of leaf, root, fruit, and flower types. (Noor et al., 2006).

Hemispherical photography techniques have been used to indirectly measure canopy cover (Dharmawan & Pramudji, 2014). Hemispherical canopy photos were taken three times for each plot, with each plot divided into five quadrants, resulting in a total of 135 canopy photos. The canopy photos were then processed using the Boolean technique. The result of this data processing is the estimated value of mangrove canopy cover and serves as the basis for grouping the mangrove vegetation conditions in each plot and sampling station.

The reference for grouping mangrove conditions is the Minister of Environment Regulation number 2001 of 2004, as presented in Table 2 (KLH, 2004).

Tabel 2. Standard Criteria and Guidelines for Determining Mangrove Damage (Kepmen LH No 201/2004).

Condition	Criteria	Canopy Cover (%)
Good	Dense	≥ 75
	Moderate	50 – 75
Damage	sparse	< 50

We use normalized difference vegetation index (NDVI) to estimate canopy cover and mangrove condition. The NDVI input is Sentinel-2A red band (band 4=665 nm) and near infrared band (band 8=842 nm), hence the formula is:

$$\boldsymbol{NDVI = \frac{(N - R)}{(N + R)}}$$

Where R is band 4 and N is band 8 of Sentinel-2A. The canopy cover measured in the field and the NDVI values extracted from each sampling plot were used as variables to develop a regression model. This model served as the basis for estimating canopy cover across the entire study area. Through this estimation, the condition of mangrove forests could be assessed over the full time series dataset. To evaluate the accuracy of estimation, the root mean square error (RMSE) was calculated by comparing the observed field measurements with the model-derived estimates.

RESULTS AND DISCUSSION

Mangrove Species and Insitu Canopy Cover

Out of a total of 323 trees observed, three species of mangroves have been identified growing in the protective mangroves of Bojo ponds, namely *Rhizophora mucronata* (n=276), *Rhizophora apiculata* (n=33), and *Sonneratia alba* (n=14). The diameter for each species was 48.7 ± 1 cm, 54.7 ± 2.7 cm, and 59.5 ± 6.1 cm, respectively. *Sonneratia alba* has a relatively larger diameter than the other

species. In addition to the three species found at the sampling stations, other mangrove species present in Bojo ponds were includes *Avicennia marina, Bruguiera gymnorhiza, Ceriops decandra, Rhizophora apiculata, R. mucronata, R. stylosa,* and *Sonneratia alba* (Saru, 2020).

Hemispherical photo analysis resulted that in June 2023, the mangrove canopy cover was 76.2 ± 5.8 percent, which is considered to be in good condition. The highest average canopy cover was found in plot 1 at 77.8 ± 3.9 percent, and the lowest in plot 3 at 75.0 ± 6.7 percent (Figure 2).

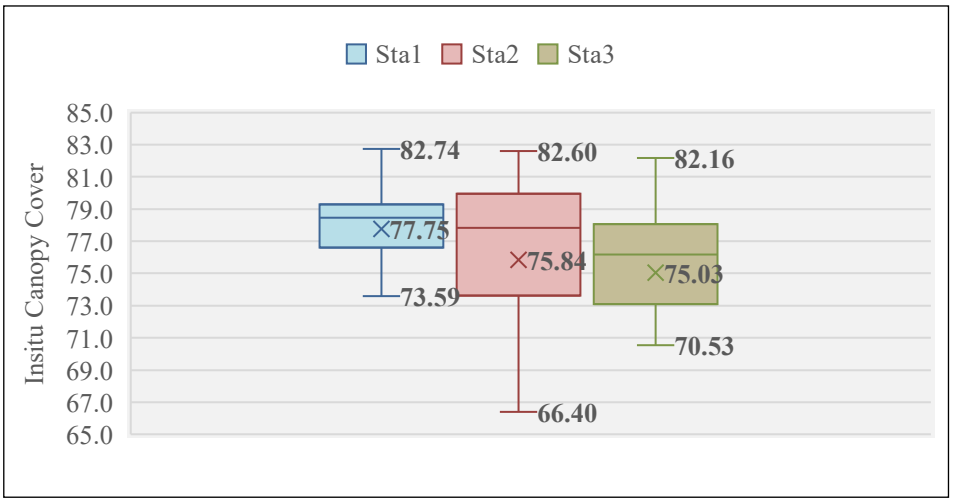

Figure 2. Canopy cover percentage from the hemispherical photo analysis of Bojo pond, June 2023.

The mangrove species commonly found in the coastal areas of South Sulawesi are *Rhizophora mucronata, Rhizophora apiculata*, and *Sonneratia alba*. These three types can be found at Tanakeke Island (Setiawan & Mursidin, 2018), Selayar Island (Selamat et al., 2020; Selamat et al., 2021), and Pannikiang Island, Barru Regency (Rusdi et al., 2020). *Sonneratia alba* can be found at Pare-pare Bay and Bone Bay, while *Rhizophora mucronata* can be found at the estuary of the Tallo River, Makassar (Setiawan, 2015) and Sinjai (Mursalim et al., 2020). In addition to *Rhizophora mucronata, Rhizophora apiculata* can also be found at Belopa, Luwu (Mutmainna et al., 2024).

According to Bosma et al. (2020), in implementing AMA (Associated Mangrove Aquaculture), which is an aquaculture system that uses mangroves as protective plants on embankments, it is important to consider the characteristics of the mangrove species being planted. Most *Rhizophora* spp. species require tidal inundation, and their propagules also grow less well in coastal areas, so they should preferably be planted along the embankments of the ponds. Meanwhile, planting mangroves on the coastal side will be more successful if using *Sonneratia alba*. Field observations show that in Bojo pond, the presence of *Sonneratia alba* is relatively low compared to *Rhizophora* spp.

Temporal NDVI, rainfall and Mangrove Conditions

Vegetation exhibits distinct reflectance characteristics in the red and near-infrared (NIR) spectral bands, which makes comparative analysis between these bands particularly effective. The normalized difference vegetation index (NDVI) is calculated by taking the difference between NIR and red reflectance values and dividing it by their sum. Low NDVI values typically represent bare soil or sparsely vegetated surfaces, while high NDVI values correspond to dense, healthy vegetation canopies (Najor et al., 1990).

The statistical regression analysis between field-derived measurements of insitu mangrove canopy cover and remotely sensed NDVI values is presented in Figure 3. The result indicates a significant positive correlation (0.91), where the derived regression model expressing canopy cover (y) as a function of NDVI (x), thereby enabling quantitative estimation of canopy density from spectral vegetation indices. The regression model is: y=68.92 x + 51.808 (n=11). The coefficient of determination (R^2) for the equation is 0.835 and The RMSE is 1.69. This model became the basis to determine NDVI threshold to estimate the condition of mangroves in Bojo, as presented in Table 3.

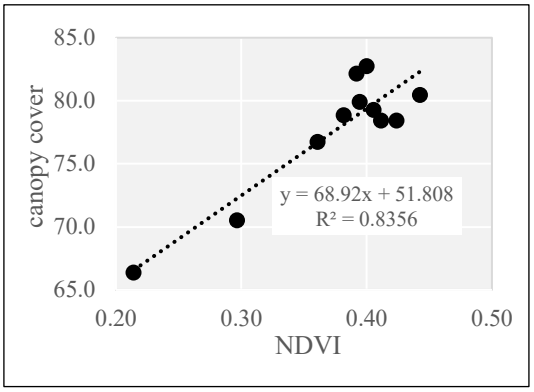

Figure 3. Regression between NDVI and in-situ canopy cover.

Table 3. NDVI Threshold Values for Estimating Mangrove Conditions

NDVI	Condition	Criteria
>0.335	Good	Dense
-0.027<NDVI<0.335		Moderate
< -0.027	Damage	sparse

NDVI values extracted from 474 Sentinel-2 images ranged from –0.12 to 0.65. Values near 1 indicate dense, healthy vegetation, whereas negative values typically reflect non-vegetated surfaces such as water bodies or mixed pixels at mangrove edges. As a comparison, a study on mangrove distribution in West Sulawesi using Sentinel-2 imagery reported NDVI values ranging from 0.06 to 0.81 (Malik et. al., 2024). Meanwhile, NDVI values on Pannikiang Island, Barru Regency, were found to range between –0.59 and 0.77 (Rosalina et. al., 2024). Figure 4 shows the recurring annual NDVI fluctuations, highlighting consistent seasonal variation in canopy cover. The highest value was recorded on 20 May 2017, and the lowest on 21 November 2016. Based on established NDVI thresholds (Table 3), the Bojo mangroves remained in good condition throughout 2016–2023.

Rainfall in the Mallusetasi District demonstrates a pronounced monsoonal pattern. Precipitation begins to increase in October–November, reaches its maximum in December, and remains elevated through January before declining in February–March. The driest conditions consistently occur during July–September. The annual rainfall distribution for 2015–2022, including the Bojo pond area, is presented in Figure 5.

Peak rainfall is observed in December–February, with values exceeding 600–800 mm in certain years, corresponding to the core rainy season. Rainfall then gradually decreases from March to May, marking the transition toward drier conditions. July–September represent the driest period, with precipitation frequently below 100–200 mm, showing the most consistent low values across years.

While the seasonal cycle is stable, interannual variability in rainfall intensity is evident. Years such as 2017 and 2020 recorded exceptionally high peaks in December–January, whereas 2019 and 2021 exhibited lower peaks, indicative of weaker rainy seasons. The mean trend confirms the general cycle: high rainfall during November–February, a decline from March–June, a minimum in July–September, and recovery in October–November.

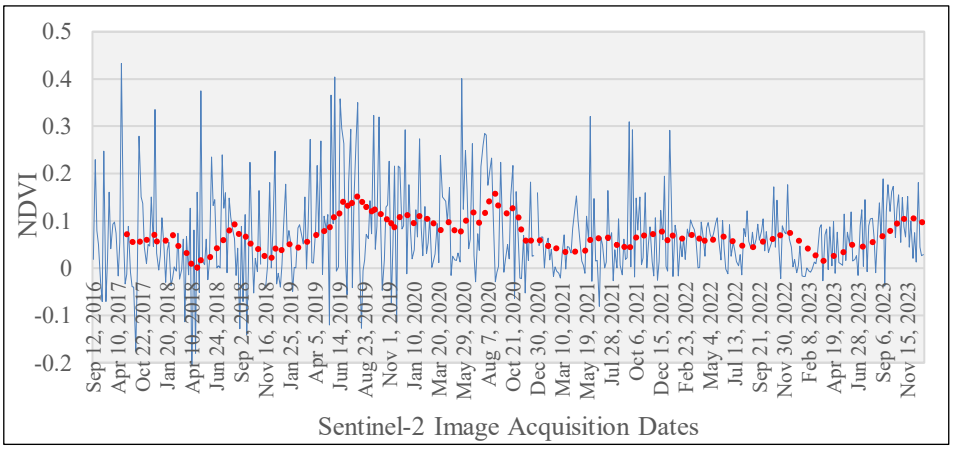

Figure 4. NDVI variations from the extraction of 474 Sentinel-2 images over the period 2016 to 2023. The red dashed line indicates the moving average trend.

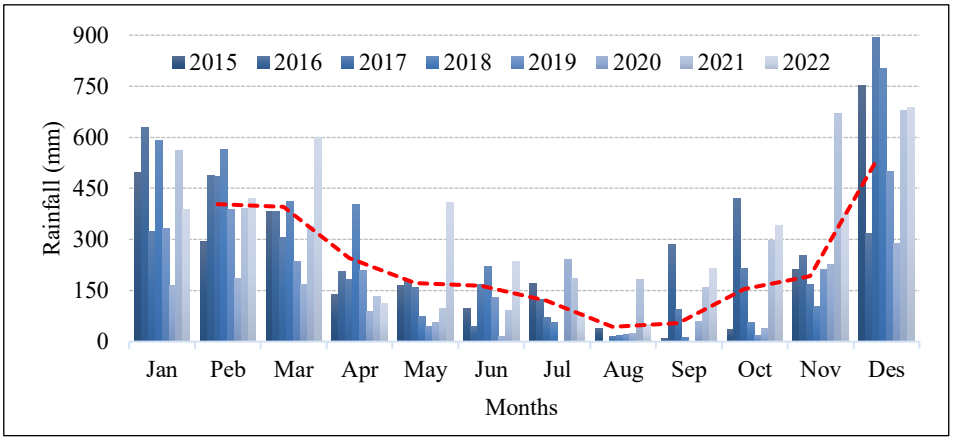

Figure 5. Monthly rainfall in Bojo throughout the year 2015 to 2022. The red dashed line indicates the moving average trend.

High rainfall conditions increase freshwater input and reduce salinity, but they may also impose stress on mangrove photosynthesis due to persistent cloud cover and reduced solar radiation. During the dry season, precipitation decreases and salinity levels rise, yet enhanced light availability creates favorable conditions for photosynthetic activity, as reflected in higher NDVI values. Interannual variability further modulates these dynamics: weaker rainy seasons tend to support higher canopy density, whereas stronger rainy seasons can temporarily suppress NDVI due to limited light penetration.

To evaluate mangrove responses, NDVI values were aggregated into two seasonal categories rainy season (November–April) and dry season (May–October). Results reveal clear seasonal variability, with lower NDVI values during the rainy season and higher values during the dry season (Figure 6). During year 2017 to 2019, NDVI values remain consistently above 0.33, indicating good mangrove condition with relatively stable canopy density. After this, NDVI begins to decline but still fluctuates around or slightly above the 0.33 threshold since year 2020 to 2021. This suggests mangroves were mostly in good condition, though signs of stress or reduced canopy density may have started to appear. At 2022, NDVI drops below 0.33, marking a shift to moderate condition. This indicates a significant reduction in canopy density or vegetation health, consistent with environmental stressors (e.g., strong rainy season, reduced sunlight, or other disturbances). Then, at 2023, NDVI values show a modest recovery, rising back toward or above the 0.33 threshold. This suggests partial improvement in mangrove condition, though not yet reaching the higher levels observed in 2017–2019.

The decline from 2020 to 2022 reflects a period of stress, possibly linked to climatic variability (heavy rainfall, cloud cover, or wind damage) or anthropogenic pressures. The recovery trend in 2023 to 2024 indicates resilience, with mangroves regaining canopy density under more favorable conditions. Overall, the chart shows that mangroves in Bojo have remained mostly in good condition, but with a notable dip to moderate condition in 2022, followed by gradual improvement. Despite remaining in generally good condition, Bojo mangroves exhibited a declining trajectory relative to 2017, with a pronounced reduction in canopy density during the dry season of 2022, followed by modest recovery in 2023. From October to December, when rainfall is elevated, NDVI values consistently decline, reflecting reduced photosynthetic capacity under high cloud cover and stronger winds that may induce leaf abscission. Conversely, during transitional and early dry season months (April–June and July–September), reduced rainfall and cloud cover enhance solar radiation, thereby promoting photosynthesis and contributing to higher NDVI values.

P-ISSN: 2460-0156
E-ISSN: 2614-5049

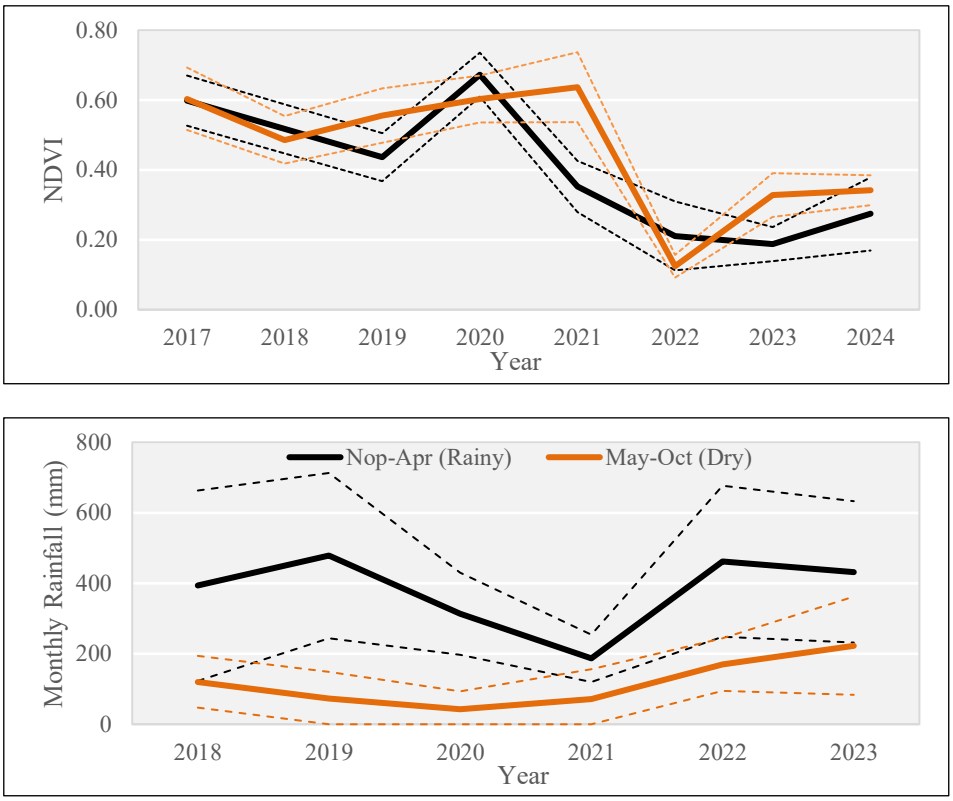

Figure 6. NDVI values extracted from Sentinel-2 during rainy and dry season from 2017 to 2023 (above) and Rainfall seasonal pattern at the same time period (below).

Results indicate that NDVI-based classification revealed distinct spatial patterns of mangrove density in the Bojo aquaculture area between 2017 and 2023 (Figure 7). Dense mangrove stands consistently occupied the landward margin of the mangrove belt, while medium-density mangroves were more frequently distributed along the seaward edge. A marked contraction of dense mangrove cover was observed in 2021 relative to preceding years. During the rainy season of 2022, the mangrove area as a whole shifted to medium-density criteria. In the rainy season of 2023, dense mangrove patches reappeared in the central portion of the area, although medium-density mangroves again dominated during the dry season of 2023. These findings highlight both the temporal variability and spatial persistence of mangrove density patterns across seasonal cycles.

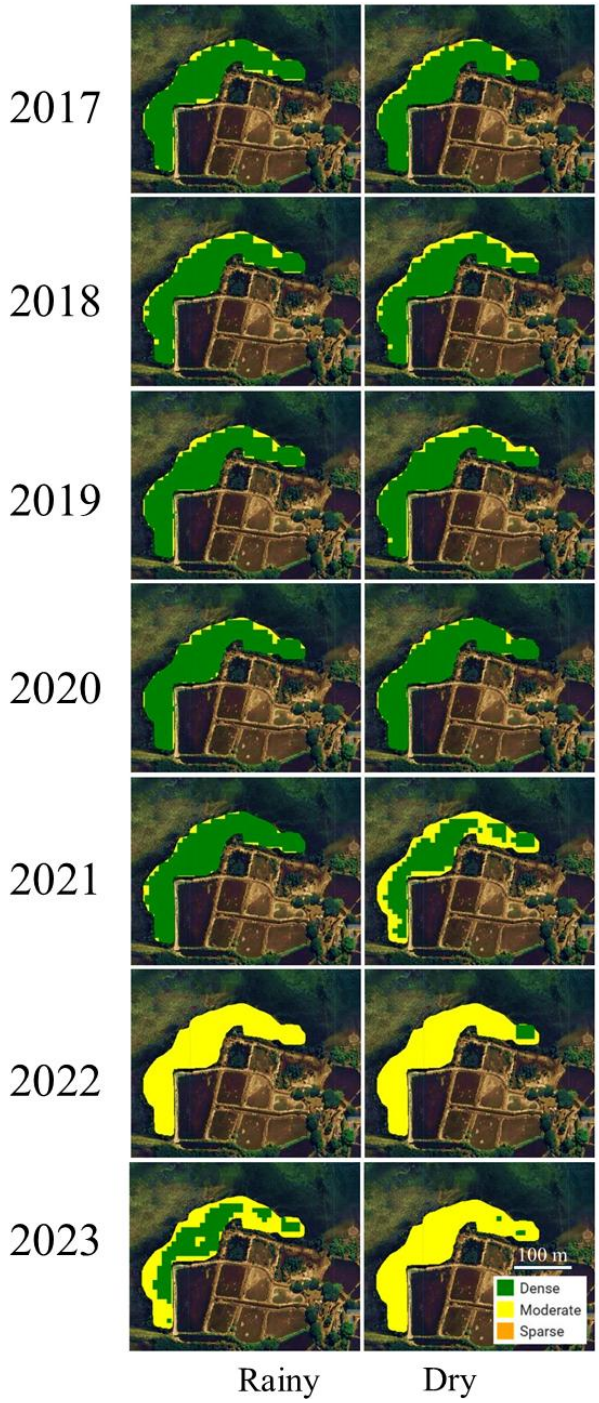

Figure 7. Spatial distribution of mangrove density classes at Bojo aquaculture ponds during rainy and dry seasons from 2017 to 2023, derived from NDVI-based canopy cover classification. The color scale represents mangrove density criteria, highlighting temporal variability and seasonal shifts in canopy cover.

Sentinel-2's 10 m spatial resolution is sufficient to capture a 2.75 ha mangrove patch, which is represented by approximately 270 pixels. Although this coverage enables broad characterization of vegetation condition, the limited pixel count constrains the detection of fine-scale structural heterogeneity. Previous studies have demonstrated that Sentinel-2 imagery is adequate for aquaculture and mangrove monitoring at pond scale, but its precision diminishes for features smaller than ~0.5 ha (Hu et al., 2024). At aquaculture pond margins, mixed pixels containing both mangrove canopy and water surface introduce spectral contamination, thereby reducing NDVI values. Moreover, seasonal variability in pond water clarity alters reflectance properties, adding noise to vegetation indices. To mitigate these effects, the integration of higher-resolution imagery is

recommended for validating edge conditions and reducing mixed-pixel bias.

CONCLUSION

The mangrove stands at Bojo as a pond protector in relatively healthy conditions, with an average canopy cover of 76%. Seasonal NDVI dynamics between 2017 and 2023 reveal a consistent pattern of higher productivity during the dry season and reduced values during the rainy season. This temporal variability indicates that mangrove vigor is tightly coupled with climatic drivers, particularly rainfall intensity and hydrological regimes. The persistence of high canopy cover suggests ecological resilience, yet the intra-annual fluctuations highlight the sensitivity of mangrove fertility to seasonal stressors.

These results emphasize the importance of integrating seasonal cycles into monitoring frameworks to capture short-term ecological variability that may otherwise be overlooked. Long-term monitoring that couples NDVI-based assessments with ground-based ecological indicators will be essential for accurate evaluation of mangrove health and for guiding conservation planning in support of sustainable aquaculture and coastal protection.

NDVI values indicate stronger canopy vigor and reduced stress during the dry season, suggesting that this period is optimal for mangrove planting, as seedling survival rates are likely to be higher. Conversely, the sensitivity of mangroves to rainy season conditions highlights the need to prioritize species tolerant of prolonged inundation and salinity fluctuations, such as *Avicennia marina* and *Sonneratia alba*, particularly along pond edges. Sentinel-2 NDVI provides a valuable tool for guiding seasonal interventions, while UAV or higher-resolution imagery can be employed to validate edge conditions and monitor seedling establishment with greater precision.

ACKNOWLEDGMENT

The authors express their sincere gratitude to the teaching assistants of the course Methods and Techniques of Marine Biological Resource Survey and to the 2020 cohort of Marine Science students at Hasanuddin University for their active participation in field data collection.

REFERENCES

Bannari, A., Morin, D., Bonn, F. & Huete, A., (1995). A review of vegetation indices. Remote sensing reviews, *13*(1-2), 95-120.

Bosma, R.H, Debrot, D., Rejeki, S., Tonneijck, F., Yuniati, A., W. & Sihombing, W. (2020). Associated Mangrove Aquaculture Farms; Building with Nature to restore eroding tropical muddy coasts. Ecoshape technical report, Dordrecht, The Netherlands.

BPS (2016). Kecamatan Mallusetasi dalam Angka 2016. Badan Pusat Statistik, Kabupaten Barru. https://barrukab.bps.go.id/publication/

BPS (2017). Kecamatan Mallusetasi dalam Angka 2017. Badan Pusat Statistik, Kabupaten Barru. https://barrukab.bps.go.id/publication/

BPS (2018). Kecamatan Mallusetasi dalam Angka 2018. Badan Pusat Statistik, Kabupaten Barru. https://barrukab.bps.go.id/publication/

BPS (2019). Kecamatan Mallusetasi dalam Angka 2019. Badan Pusat Statistik, Kabupaten Barru. https://barrukab.bps.go.id/publication/

BPS (2020). Kecamatan Mallusetasi dalam Angka 2020. Badan Pusat Statistik, Kabupaten Barru. https://barrukab.bps.go.id/publication/

BPS (2021). Kecamatan Mallusetasi dalam Angka 2021. Badan Pusat Statistik, Kabupaten Barru. https://barrukab.bps.go.id/publication/

BPS (2022). Kecamatan Mallusetasi dalam Angka 2022. Badan Pusat Statistik, Kabupaten Barru. https://barrukab.bps.go.id/publication/

BPS (2023). Kecamatan Mallusetasi dalam Angka 2023. Badan Pusat Statistik, Kabupaten Barru. https://barrukab.bps.go.id/publication/

Díaz, B. M., & Blackburn, G. A. (2003). Remote sensing of mangrove biophysical properties: Evidence from a laboratory simulation of the possible effects of background variation on spectral vegetation indices. International Journal of Remote Sensing, 24(1), 53–73. https://doi.org/10.1080/01431160305012

European Space Agency (ESA) 2015 Sentinel-2 User Handbook vol 64

Furusawa, T., Koera, T., Siburian, R., Wicaksono, A., Matsudaira, K., and Ishioka, Y. (2023). Time-series analysis of satellite imagery for detecting vegetation cover changes in Indonesia. Scientific reports, 13(1), 8437.

Hu, Y., Zhang, L., Chen, B., & Zuo, J. (2024). An object-based approach to extract aquaculture ponds with 10-meter resolution Sentinel-2 images: a case study of Wenchang City in Hainan Province. Remote Sensing, 16(7), 1217.

https://earthengine.google.com/platform/. accessed June 2024

https://sentiwiki.copernicus.eu/web/s2-applications, accessed June 2024.

Dharmawan, I. W. E., & Pramudji (2014) Panduan monitoring status ekosistem mangrove, Jakarta: Pusat Penelitian Oseanografi, Lembaga Ilmu Pengetahuan Indonesia and PT. Sarana Komunikasi Utama

Jamaluddin, I., Chen, Y. N., Ridha, S. M., Mahyatar, P., & Ayudyanti, A. G. (2022). Two decades mangroves loss monitoring using random forest and landsat data in east luwu, indonesia (2000–2020). Geomatics, *2*(3), 282-296.

Kementerian Lingkungan Hidup (2004) Keputusan Menteri Lingkungan Hidup No. 201 tahun 2004 Kriteria baku dan pedoman penentuan kerusakan mangrove (Indonesia)

Major, D.J., Baret, F.E.D.E. & Guyot, G., (1990). A ratio vegetation index adjusted for soil brightness. International journal of remote sensing, *11*(5), 727-740.

Malik, A., Ali, M.I., Jalil, A. R., Zhiddiq, S., Mannan, A., & Musyawarah, R. 2024. Monitoring Sebaran dan Kerapatan Mangrove Menggunakan Transformasi NDVI pada Citra Sentinel-2 di Provinsi Sulawesi Barat. Jurnal Environmental Science, *6*(2), 75-84.

Mursalim, A., Nurdin, N., La Nafie, Y., Selamat, B., Tresnati, J. & Tuwo, A., (2020), March. Mangrove area and vegetation condition resulting from the planting of mangroves in the Wallacea Region, Bone Bay, South Sulawesi. In IOP Conference Series: Earth and Environmental Science (Vol. 473, No. 1, p. 012055). IOP Publishing.

Mutmainna, N., Umar, M. & Salam, M.A., (2024). Estimasi Simpanan Karbon Tegakan *Rhizophora spp*., Dan Sedimen Ekosistem Mangrove Di Kecamatan Belopa, Kabupaten Luwu. Bioma: Jurnal Biologi Makassar, *9*(1), 145-159.

Naylor, R.L., Goldburg, R.J., Primavera, J.H., Kautsky, N., Beveridge, M.C., Clay, J., Folke, C., Lubchenco, J., Mooney, H & Troell, M., (2000). Effect of aquaculture on world fish supplies. Nature, 405(6790), 1017-1024.

Noor, R., Khazali, M., & Suryadiputra, I. N. N. (2006) Panduan Pengenalan Mangrove Di Indonesia (Bogor: PHKA/WI-IP).

Rosalina, D., Sabilah, A. A., Rombe, K. H., & Warni, W. (2024). Mapping of Mangrove Conditions Using Sentinel-2 Imagery. JST (Jurnal Sains dan Teknologi), *13*(1), pp. 89-98.

Ruan, L., Yan, M., Zhang, L., Fan, X., & Yang, H. (2022). Spatial-temporal NDVI pattern of global mangroves: A growing trend during 2000–2018. Science of the Total Environment, 844, 157075.

Rusdi, R., Setyobudiandi, I. & Damar, A., (2020). Kajian potensi dan pengelolaan berkelanjutan ekosistem mangrove Pulau Pannikiang, Kabupaten Barru, Sulawesi Selatan. Jurnal Ilmu dan Teknologi Kelautan Tropis, *12*(1), 119-133.

Saru, A., (2020). Korelasi antara Kepadatan Makrozoobentos dengan Kandungan Karbon pada Ekosistem Mangrove di Kawasan Tambak Pendidikan Unhas. Prosiding Simposium Nasional Kelautan dan Perikanan, 7.

Selamat, M.B., Mashoreng, S., Amri, K. & Rappe, R.A., (2020), September. The use of sentinel 2A imageries to improve mangrove inventarization at coremap CTI monitoring areas. In IOP Conference Series: Earth and Environmental Science (Vol. 564, No. 1, p. 012065). IOP Publishing.

Selamat, M.B., Mashoreng, S., Amri, K., Rappe, R.A. & Jompa, J., (2021), October. Mangrove condition at Selayar Island based on field data and NDVI. In IOP Conference Series: Earth and Environmental Science (Vol. 860, No. 1, p. 012084). IOP Publishing.

Setiawan, H., & Mursidin. (2018). Ecological Characteristic and Health of Mangrove Forest at Tanakeke Island South Sulawesi. Jurnal Penelitian Kehutanan Wallacea, 7(1), pp. 47-58.

Setiawan, H., 2015. Akumulasi dan distribusi logam berat pada vegetasi mangrove di pesisir Sulawesi Selatan. Jurnal Ilmu Kehutanan, 7(1), pp.12-24.

Tran, T. V., Reef, R., & Zhu, X. (2022). A review of spectral indices for mangrove remote sensing. Remote Sensing, *14*(19), 4868.

Win, K. S., and Sasaki, J. (2024). The change detection of mangrove forests using deep learning with medium-resolution satellite imagery: A case study of Wunbaik Mangrove Forest in Myanmar. Remote Sensing, *16*(21), 4077.

Xue, J., & Su, B. (2017). Significant remote sensing vegetation indices: A review of developments and applications. Journal of sensors, 2017(1), p.1353691.

Appendix 1. GEE Script to mapping NDVI time series from 2016 to 2023

```
// ###################################
// # Script GEE untuk menghitung variasi NDVI mangrove
// # hasil modifikasi
// ###################################
// # 1) Menampilkan ROI
// ###################################
Map.addLayer(geometry)
Map.centerObject(geometry)

// ###################################
// # 2) menyaring koleksi citra
// # memanggil data Sentinel-2
// # filter menurut tanggal dan ROI
// # cetak daftar citra di konsol
// ###################################
var s2 = ee.ImageCollection('COPERNICUS/S2')
 var collection = ee.ImageCollection('COPERNICUS/S2')
                .filterDate('2016-08-31', '2023-12-31')
                .filterBounds(geometry)
                .filter(ee.Filter.lt('CLOUDY_PIXEL_PERCENTAGE',10))
print(collection)
// ###################################
// # 3) menyaring koleksi citra
// # filter menurut tanggal dan ROI
// # hitung median
// ###################################

var filtered = s2.filter(ee.Filter.lt('CLOUDY_PIXEL_PERCENTAGE', 10))
  .filter(ee.Filter.date('2016-08-31', '2023-12-31'))
  .filter(ee.Filter.bounds(geometry))

var image = filtered.median();
var klip = image.clip(geometry);

var filtered17 = s2.filter(ee.Filter.lt('CLOUDY_PIXEL_PERCENTAGE', 10))
  .filter(ee.Filter.date('2017-01-31', '2017-12-31'))
  .filter(ee.Filter.bounds(geometry))

var image17 = filtered17.median();
var klip17 = image17.clip(geometry);

var filtered22 = s2.filter(ee.Filter.lt('CLOUDY_PIXEL_PERCENTAGE', 10))
  .filter(ee.Filter.date('2022-01-31', '2022-12-31'))
  .filter(ee.Filter.bounds(geometry))

var image22 = filtered22.median();
var klip22 = image22.clip(geometry);

// ################################################
// # 4) Fungsi hitung Normalized Difference Vegetation Index (NDVI)
// # 'NIR' = B8 dan 'RED' = B4
// # Fungsi ini akan menambahkan band NDVI pada citra Sentinel-2.
// ################################################

var addNDVI = function(image) {
  var ndvi = image.normalizedDifference(['B8', 'B4']).rename('ndvi');
```

```
  return image.addBands(ndvi);
};

var withNDVI = s2.filterDate('2016-08-31', '2023-12-31')
    .map(addNDVI); // <-- map() the function over the collection.

// ##########################################
// # 5) Membuat Grafik
// # menampilkan NDVI runtun waktu
// # sesuai batas waktu koleksi data
// ##########################################
var chart = ui.Chart.image.series({
  imageCollection: withNDVI.select('ndvi'),
  region: geometry, //ROI bisa diset sesuai sta sampling
  reducer: ee.Reducer.first(),
  scale: 10
});

// ##########################################
// # Mendefinisikan opsi untuk tampilan grafik
// # cek link:https://developers.google.com/chart/interactive/docs/reference
// ##########################################
var options = {
  title: 'NDVI over time',
  hAxis: { title: 'time' },
  vAxis: { title: 'NDVI' },
  series: {
    0: { color: 'red' }
  }
};

// ######################################
// # Atur grafik dan tampilkan di konsol
// ######################################
chart = chart.setOptions(options);
print(chart); // Put it in the console

// ######################################
// # Skala ulang tampilan nilai NDVI
// ######################################
var withNdvi = filtered.map(addNDVI);

var composite = withNdvi.median()
var ndviComposite = composite.select('ndvi').clip(geometry)

var palette = [
  'FFFFFF', 'CE7E45', 'DF923D', 'F1B555', 'FCD163', '99B718',
  '74A901', '66A000', '529400', '3E8601', '207401', '056201',
  '004C00', '023B01', '012E01', '011D01', '011301'];

var addNDVI = {min:0, max:1.0, palette: palette }
Map.addLayer(ndviComposite, addNDVI, 'ndvi')

// menampilkan citra komposit RGB di peta
Map.addLayer(klip,{bands:['B4','B3','B2'], min:750, max:2990}, "Natural-colour");
// menampilkan citra komposit RGB di peta
Map.addLayer(klip,{bands:['B8','B11','B5'], min:750, max:2990}, "False-colour");
```

```
// menampilkan citra komposit RGB di peta
Map.addLayer(klip17,{bands:['B8','B11','B5'], min:750, max:2990}, "False-colour17");

// menampilkan citra komposit RGB di peta
Map.addLayer(klip22,{bands:['B8','B11','B5'], min:750, max:2990}, "False-colour22");

//selesai.
```